High-resolution soft X-ray measurements in slow Ne^{9+} ions transmitted through a microcapillary

Yoshio Iwai,[*1,*2] Sebastien Thuriez,[*1] Yasuyuki Kanai,[*1] Hitoshi Oyama,[*1] Kozo Ando,[*1] Roger Hutton,[*1,†] Hideki Masuda,[*3] Kazuyuki Nishio,[*3] Ken-ichiro Komaki,[*2] and Yasunori Yamazaki[*1,*2]

[*1] *Atomic Physics Laboratory, RIKEN*

[*2] *Institute of Physics, Graduate School of Arts and Sciences, University of Tokyo*

[*3] *Department Industrial Chemistry, Tokyo Metropolitan University*

X-ray emitted from 2.3 keV/u Ne^{9+} ions transmitted through a thin Ni microcapillary foil were measured with a new high-resolution soft X-ray spectrometer. It is found electronic core configuration of excited He-like and Li-like ions with *K* hole.

Introduction

When a slow highly charged ion approaches a solid surface, the ion is accelerated toward the surface with its image potential and then the ion resonantly captures target valence electrons into its excite states. Such an atom (ion) with multiply excited electrons and inner shell vacancies is called a "hollow atom"(ion).[1–10] The formation and relaxation dynamics of hollow atoms above and bellow the surface, have been studied intensively in recent years, *e.g.*, Briand *et al.* observed X-rays emitted from Ar^{17+} ions impinging on a Ag target with a crystal spectrometer.[1] However, an existence time of the hollow atom above the surface is limited, typically 10^{-13}–10^{-14}sec., which is normally shorter than its intrinsic lifetime. To avoid the difficulty, the hollow atom is extracted *in vacuum* employing a microcapillary target.[11–14] Ninomiya *et al.* observed X-rays emitted from ions downstream of a Ni microcapillary target for 9 keV/u Ne^{9+} ions with a Si(Li) detector.[15] The peak energy of *KL* transitions measured for the capillary target was about 50 eV higher than that for a flat surface target, indicating that the observed exited states are quite different between the two targets. Lifetimes of excited states produced with the capillary target were found to be order of nanoseconds, which is much longer than a typical lifetime of the Ne *K* hole.[13] However, the energy resolution of the Si(Li) detector (∼100 eV at 900 eV) is not enough to identify the electronic configurations and the number of electrons in outer shells during X-ray emission, which is expected to be very important to understand the dynamics of the hollow atom formation and relaxation processes. In order to obtain relevant information described above, we have developed a high-resolution grating soft X-ray spectrometer.

Experimental

We used a 14.5 GHz Caprice type electron cyclotron resonance (ECR) ion source in RIKEN. As is shown in Fig. 1,

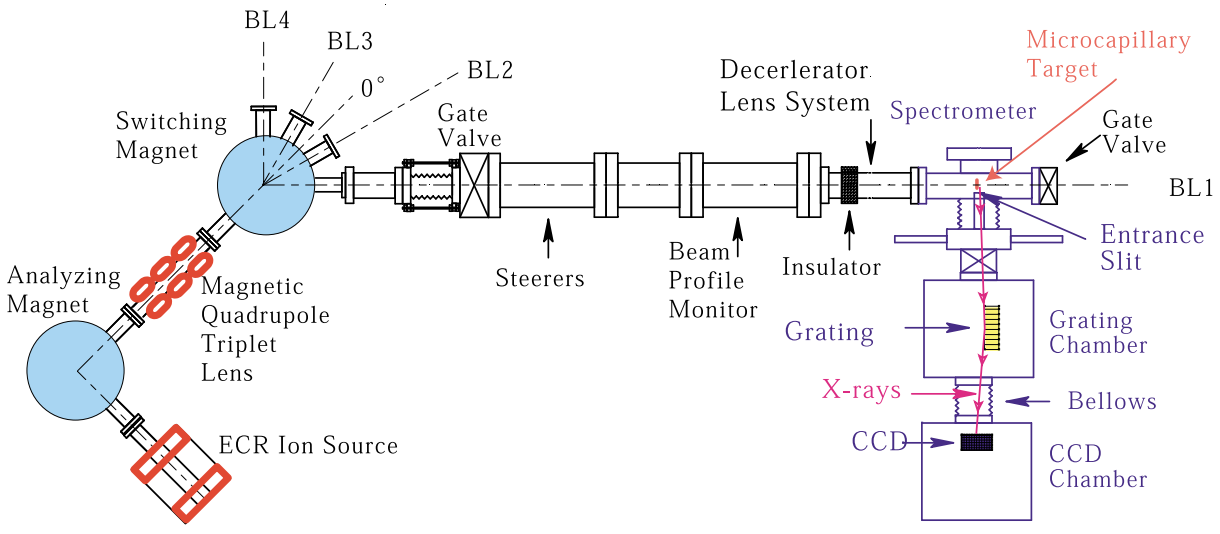

Fig. 1. Schematic drawing of experimental configuration.

† Present address: Department of Physics, University of Lund, Sweden

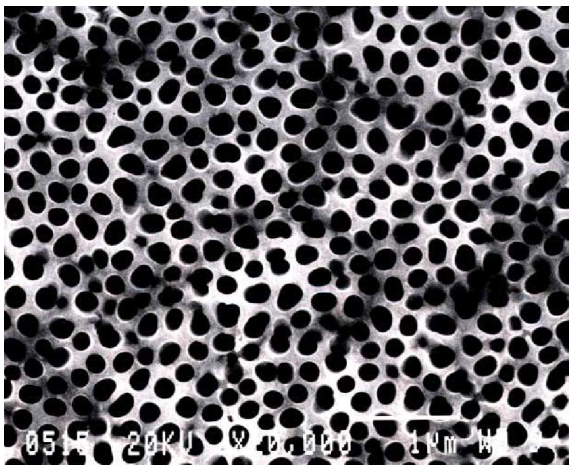

Fig. 2. Image of Ni microcapillary (taken by SEM).

a slow highly charged ion beam was extracted from the ECR ion source and momentum-analyzed by an analyzing magnet. The beam was focused by a magnetic quadrupole triplet lens and delivered to the beam line (BL1) *via* a switching magnet. The analyzing magnet, switching magnet and all beam lines can be floated so that very slow highly charged ions can be delivered effectively to the target chamber which is at the ground potential.[16] The ion beam was adjusted by steers, monitored with a beam profile monitor and focused at a target position with a deceleration lens system. The microcapillary target was $\sim$1 mm^2 in size with a thickness of $\sim$1 μm and had a multitude of straight holes of $\sim$200 nm in diameter. Figure 2 shows a scanning electron microscope image of the Ni capillary target. X-rays emitted from the ions at the target downstream were observed with the spectrometer, which was installed perpendicular to the ion beam. The spectrometer consists of three parts, a target chamber, a grating chamber, and a CCD (Charge Coupled Device) chamber, as shown in Fig. 3. The target mounted on an X-Y stage is movable perpendicular and parallel to the ion beam. An electron gun is installed in the target chamber to produce X-rays, which are used to calibrate the spectrometer. The target and grating chambers are separated by an entrance slit of 25 μm where X-rays pass through to the grating chamber. Two baffles are prepared along the X-ray path to reduce stray lights. The grating (HITACHI, parts No.001-0450) with varied groove spacing is designed for a grazing-incidence spectrometer in which diffracted X-rays focus onto a plane (focal

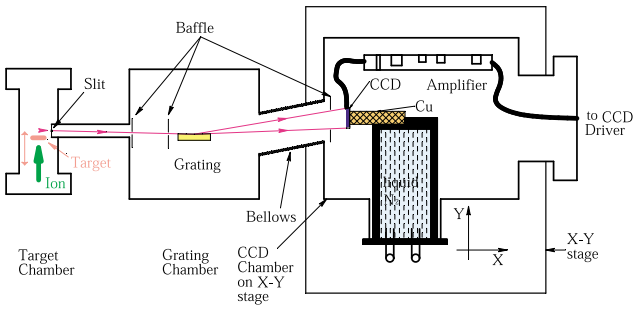

Fig. 3. Schematic drawing of the high-resolution soft X-ray spectrometer.

Table 1. Specifications of grating, entrance slit, and CCD.

Grating	
Lattice space	1/2,400 mm
Width × height × thickness	50 mm × 30 mm × 10 mm
Blaze angle	1.9°
Incident angle	88.65°
Energy range	200∼1,200 eV
Radius of curvature	15,290 mm
Coating	Au
Slit	
Width × Height	25 μm × 5 mm
CCD	
Pixel size	26 μm × 26 μm
Pixel format	1,024 × 255
Image area	26.6 mm × 6.7 mm
Readout noise (at 233 K, 20 kHz)	6electrons (r. m. s.)
Dark signal (at 150 K)	10^{-5}electrons/pixels/seconds
Output amplifier gain	1.5 μV/electrons

plane) that is almost normal to the X-rays.[17] A baffle blocks reflected lights to reach the CCD. Diffracted X-rays are detected by a back-illuminated CCD (EEV CCD30-11), which is operated at 150 K cooling by liquid N_2 to reduce a dark signal. The CCD chamber stands on an X-Y stage to adjust the CCD position to the focal plane. Various parameters of the spectrometer are summarized in Table 1.

The grating equation is

$$m\lambda = d(\sin\alpha - \sin\beta), \tag{1}$$

where m is an order of diffraction, λ is a wavelength of X-rays, α and β are an incident angle and a diffraction angle, respectively. The grating is a mechanically ruled aberration-corrected concave one, which needs a unique arrangement as shown in Fig. 4. The plane A is the tangent plane of the grating surface at its center, the focal plane is then perpendicular to the plane A at L from the grating center. The relation between the diffraction angle and distance y measured from the intersection **P**, along the focal plane is given by

$$y = \frac{L}{\tan\beta}. \tag{2}$$

From Eqs. (1) and (2), the energy dispersion is given by

$$\Delta E = C\frac{L}{d(\sin i - \frac{C}{Ed})^2\sqrt{1-(\sin i - \frac{C}{Ed})^2}}\Delta y, \tag{3}$$

where C is a transform constant of energy and wave length and E is an X-ray energy. As is seen from Eq.(3), the energy

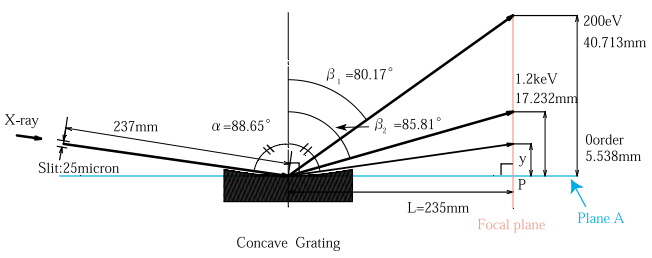

Fig. 4. Schematic drawing of the characteristic optical path of the grating for soft X-ray with the focal plane.

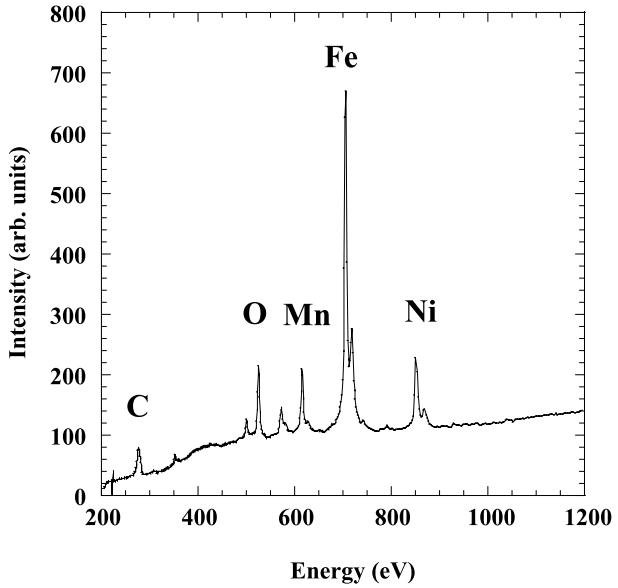

Fig. 5. Spectrum of stainless steel target with 4 keV electron impact, measured with the spectrometer.

resolution is limited by the pixel size and approximately by the slit width. X-rays emitted from a stainless steel plate with 4 keV electron impact, were observed. Figure 5 shows L X-rays of Ni, Fe, Mn, and K X-rays of O, C.[18)]

These peaks were used for calibration. The full width at half maximum of Fe $L\alpha$ peak was 3pixels, which is 7.6 eV at 900 eV and 1.4 eV at 300 eV from Eq.(3). The energy resolution as a function of the X-ray energy is given in Fig. 6. It is possible to take a decay curve by moving the capillary target, which is mounted on the X-Y stage along the ion beam. The observed region along the ion trajectory is almost the same as the slit width, 25 μm, which corresponds to the time range of 37picoseconds at 2.3 keV/u ions.

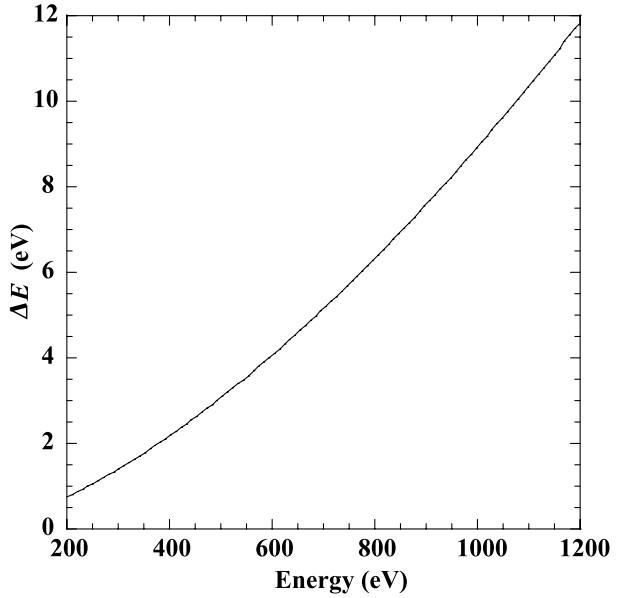

Fig. 6. Energy resolution (FWHM) dependences on X-rays energy of the spectrometer.

Results and discussion

The red and black solid lines in Fig. 7 show the Ne $K\alpha$ X-ray spectrum taken with the spectrometer for 2.3 keV/u Ne^{9+} ions transmitted through the Ni capillary and that directly hitting a flat stainless steel plate at ∼30degrees from the surface normal, respectively. To compare, the red and black dashed lines show the spectrum taken with a windowless Si(Li) detector for 9 keV/u Ne^{9+} ions transmitted through the Ni capillary and that directly hitting a flat Al plate, respectively.[15)] The peak energy for the stainless steel target is observed at 849.5±1.3 eV, which is identified to Ne $K\alpha$ X-rays predicted to appear at 848.6 eV. It is seen that the peak skews to high-energy side indicating contributions from different number of L-shell vacancies. In the case of the capillary target, three sharp peaks were observed at 921.7±1.3 eV, 913.4±1.3 eV, and 895.4±1.3 eV. A comparison with theoretical calculation and reference data shows that the three peaks are attributed to core electronic transitions of He-like 1s2p $^1P_1 \rightarrow 1s^2\ ^1S_0$ (922.1 eV), 1s2p $^3P_1 \rightarrow 1s^2\ ^1S_0$ (914.9 eV), and Li-like 1s2s2p $^4P_{1/2,3/2} \rightarrow 1s^2 2s\ ^2S_{1/2}$ (895.0 eV), respectively.[13,19)] The observed transitions with their core configurations are summarized in Table 2.

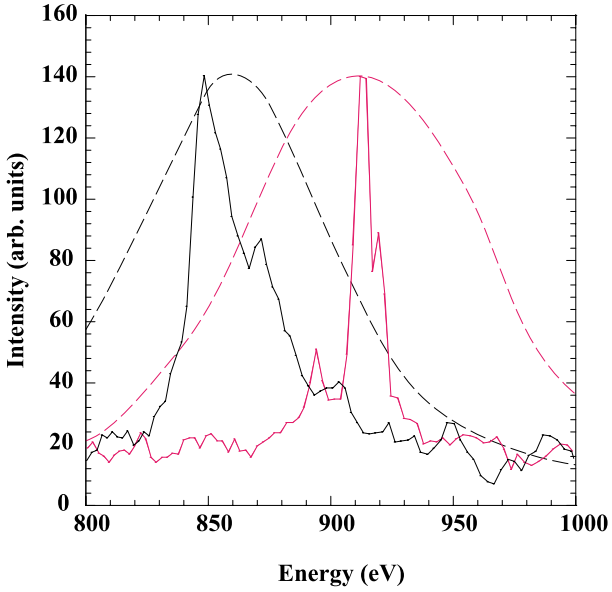

Fig. 7. Spectra of K X-rays measured with the spectrometer, for 2.3 keV/u Ne^{9+} ions transmitted through a Ni capillary (red solid line), and those hit with a stainless steel plate (black solid line). Spectra of K X-rays measured with Si(Li) detector, for 9 keV/u Ne^{9+} ions transmitted through a Ni capillary (red dashed line), and those hit with an Al plate (black dashed line) are shown for comparison.

Table 2. Electronic core configurations.

Experiment	Ref. data	Configuration	Term
913.4±1.3 eV	914.9 eV[17)]	1s2p → $1s^2$	$^3P_1 \rightarrow {}^1S_0$
921.7±1.3 eV	922.1 eV[17)]	1s2p → $1s^2$	$^1P_1 \rightarrow {}^1S_0$
895.4±1.3 eV	895.0 eV[13)]	1s2s2p → $1s^2$2s	$^4P_{1/2} \rightarrow {}^2S_{1/2}$
			($^4P_{3/2} \rightarrow {}^2S_{1/2}$)

Conclusions

We have developed a soft X-ray grating high-resolution spectrometer. Its energy resolution was 7.6 eV at 900 eV, 1.4 eV at 300 eV (FWHM), with the energy accuracy of ±1.3 eV at 900 eV, ±0.5 eV at 300 eV and the time resolution of 37picoseconds with 2.3 keV/u ion. X-rays emitted from ions transmitted through a thin Ni microcapillary foil were measured. Electronic core configurations are determined with the spectroscopy of hollow atoms using the high-resolution soft X-ray spectrometer. We are preparing a single photon counting CCD system, which allows, in principle, a noise free high-resolution spectroscopy in the soft X-ray region. It is expected that very important information will be available to understanding the dynamics of the hollow atom formation and relaxation processes.

References

1) J. P. Briand, L. de Billy, P. Charles, and S. Essabaa: Phys. Rev. Lett. **65**, 159 (1990).
2) F. W. Meyer, S. H. Overbury, C. C. Havener, P. A. Zeijlmans van Emmichoven, and D. M. Zehner: Phys. Rev. Lett. **67**, 723 (1991).
3) H. J. Andrae et al.: Z. Phys. D **21**, S135 (1991).
4) HP. Winter: Europhys. Lett. **18**, 207 (1992).
5) J. Das and R. Morgenstern: Phys. Rev. A **47**, R755 (1993).
6) F. Aumayr, H. Kurz, D. Schneider, M. A. Briere, J. W. McDonald, C. E. Cunningham, and HP. Winter: Phys. Rev. Lett. **71**, 1943 (1993).
7) R. Koehrbrueck, M. Grether, A. Spieler, and N. Stolterfoht: Phys. Rev. A **50**, 1429 (1994).
8) L. Folkerts, S. Schippers, D. M. Zehner, and F. W. Meyer: Phys. Rev. Lett. **74**, 2204 (1995).
9) K. Kakutani, T. Azuma, Y. Yamazaki, K. Komaki, and K. Kuroki: Jpn. J. Appl. Phys. **34**, L580 (1995).
10) T. Neidhart, F. Pichler, F. Aumayr, HP. Winter, M. Schmid, and P. Varga: Phys. Rev. Lett. **74**, 5280 (1995).
11) H. Masuda and K. Fukuda: Science **268**, 1466 (1995).
12) H. Masuda and M. Satoh: Jpn. J. Appl. Phys. **35**, L126 (1996).
13) Y. Yamazaki, S. Ninoimya, F. Koike, H. Masuda, T. Azuma, K. Komaki, K. Kuroki, and M. Sekiguchi: J. Phys. Soc. Jpn. **65**, 1199 (1996).
14) S. Ninomiya, Y. Yamazaki, F. Koike, H. Masuda, T. Azuma, K. Komaki, K. Kuroki, and M. Sekiguchi: Phys. Rev. Lett. **78**, 4557 (1997).
15) S. Ninomiya, Y. Yamazaki, T. Azuma, K. Komaki, F. Koike, H. Masuda, K. Kuroki, and M. Sekiguchi: Physica Scripta T **73**, 316 (1997).
16) Y. Kanai, D. Dumitriu, Y. Iwai, T. Kambara, M. Kitajima, T. M. Kojima, A. Mohri, Y. Morishita, Y. Nakai, N. Oshima, H. Oyama, M. Wada, and Y. Yamazaki: RIKEN Rev., No. 31, p. 62 (2000).
17) N. Nakano, H. Kuroda, T. Kita, and T. Harada: Appl. Opt. **23**, 2386 (1984).
18) Peak of C *KL* transition is broader than the other peaks.
19) R. L. Kelly: J. Phys. Chem. Ref. Data, **16** Suppl. 1 (1987).